Anal. Chem. **1998,** *70,* 2115−2122

Correlation of Supercritical Fluid Extraction with Supercritical Fluid Chromatography in Aqueous Matrixes

Tiing Yu,* Sheng-Kang Luo, and Shin Jyh Chen

Department of Applied Chemistry, National Chiao Tung University, Hsinchu, Taiwan, Republic of China

A mathematical model is presented for correlating supercritical fluid chromatography (SFC) in aqueous stationary phases with supercritical fluid extraction (SFE) in aqueous matrixes. A solar coaxial countercurrent chromatography apparatus was used for the SFC and SFE experiments. The SFE extraction vessel, i.e., the column for SFC, was mathematically divided into limited layers. During extraction, each layer was considered to undergo a chromatographic process. The plate heights of all the layers were regarded equal throughout the column because pressure drops in the system were negligible. Each layer's chromatographic capacity factor and peak width were calculated using true SFC experimental data, and the sum of all these peak distributions as a function of time gave the extraction efficiency. Accordingly, the SFE analyte recovery curve could be simulated using SFC data and this model. Since SFC operations are more straightforward than SFE operations, SFE optimization may be more easily achieved using this mathematical correlation. The simulated analyte data of large capacity factors matched the experimental results very well. Deviations gradually became greater as analyte capacity factors were decreased. A rationale is proposed that satisfactorily interprets this deviation trend.

The supercritical fluid extraction (SFE) technique has developed rapidly for solid-sample preparation in chemical analysis. It has drawn attention comparable to that given other techniques, such as Soxhlet and sonication extractions.[1,2] SFE applications include very broad areas, such as extraction of pesticides and herbicides from soil and animal tissues[3−5] and extraction of chlorinated hydrocarbons[6−8] and polycyclic aromatic hydrocarbons[9−11] from various environmental matrixes. SFE has also been applied to natural product analyses and semipreparations.[12,13] In addition to working with solid matrixes, it also shows potential for directly extracting analytes from liquid samples, especially from aqueous samples.[14−16] Although SFE has mainly been applied to nonpolar compounds, studies on metal extraction from solid and liquid matrixes using chelating agents have drawn a great deal of attention.[17−19] Proteins were reported to form reverse micelles[20] and have been extracted from aqueous solutions using supercritical fluid carbon dioxide (SF CO_2) with fluorinated surfactants. The solvation power of supercritical fluids can be controlled by varying pressure and temperature. Supercritical fluids, such as CO_2, become gases under ambient conditions; therefore, no further concentration is needed to separate effluents from analytes of interest. These advantages make SFE an attractive alternative to conventional liquid extraction techniques.

Since solid-matrix extraction has been a major interest for years, a large body of research can be found in the literature.[21] However, factors that influence the extraction process involve so many parameters that optimization of SFE is usually carried out on experimental data using factorial or simplex designs.[22−24] Some fundamental studies have been done in order to provide more extensive knowledge of the extraction process. A kinetic model proposed by Pawliszyn[25] considered mass transfer from the matrix

(1) Hawthorne, S. B.; Miller, D. J. *Anal. Chem.* **1994**, *66*, 4005−4012.
(2) Lopez-Avila, V.; Young, R.; Benedicto, J.; Ho, P.; Kim, R.; Beckert, W. F. *Anal. Chem.* **1995**, *67*, 2096−2102.
(3) van der Velde, E. G.; Ramlal, M. R.; van Beuzekom, A. C.; Hoogerbrugge, R. *J. Chromatogr.* **1994**, *683*, 125−139.
(4) Snyder, J. M.; King, J. W.; Rowe, L. D.; Woerner, J. A. *J. AOAC Int.* **1993**, *76*, 888−892.
(5) Tena, M. T.; Luque de Castro, M. D.; Valcarcel, M. *Chromatographia* **1995**, *40*, 197−203.
(6) Sterzenbach, D.; Wenclawiak, B. W.; Weigelt, V. *Anal. Chem.* **1997**, *69*, 831−836.
(7) Langenfeld, J. J.; Hawthorne, S. B.; Miller, D. J.; Pawliszyn, J. *Anal. Chem.* **1995**, *67*, 1727−1736.
(8) Vanbavel, B.; Jaremo, M. Karlsson, L.; Lindstrom, G. *Anal. Chem.* **1996**, *68*, 1279−1283.
(9) Champagne, A. T.; Bienkowski, P. R. *Sep. Sci. Technol.* **1995**, *30*, 1289−1307.
(10) Hawthorne, S. B.; Miller, D. J. *Anal. Chem.* **1994**, *66*, 4005−4012.
(11) Barnabas, I. J.; Dean, J. R.; Tomlinson, W. R.; Owen, S. P. *Anal. Chem.* **1995**, *67*, 2064−2096.
(12) Sargenti, S. R.; Lancas, F. M. *J. Chromatogr.* **1994**, *667*, 213−218.
(13) Chun, M.-K.; Shin, H.-W.; Lee, H.; Liu, J.-R. *Biotechnol. Tech.* **1994**, *8*, 547−550.
(14) Hedrick, J.; Taylor, L. T. *Anal. Chem.* **1989**, *61*, 1986−1988.
(15) Thiebaut, D.; Vannoort, R. W.; Brinkman, U. A. Th.; Chervet, J. P.; De Jong, G. J.; Frei, R. W. *J. Chromatogr.* **1989**, *477*, 151−159.
(16) Barnabas, I. J.; Dean, J. R.; Hitchen, S. M.; Owen, S. P. *J. Chromatogr., A* **1994**, *665*, 307−315.
(17) Lin, Y.; Wai, C. M. *Anal. Chem.* **1994**, *66*, 1971−1975.
(18) Wang, J.; Marshall, W. D. *Anal. Chem.* **1994**, *66*, 1658−1663.
(19) Wai, C. M.; Wang, S. F.; Liu, Y.; Lopez-Avila, V.; Beckert, W. F. *Talanta*, **1996**, *43*, 2083−2091.
(20) Johnston, K. P.; Harrison, K. L.; Clarke, M. J.; Howdle, S. M.; Heitz, M. P.; Bright, F. V.; Carlier, C.; Randolph, T. W. *Science* **1996**, *271*, 624−626.
(21) Chester, T. L.; Pinkston, J. D.; Raynie, D. E. *Anal. Chem.* **1996**, *68*, 487R−514R.
(22) Maio, O.; Vonholst, C.; Wenclawiak, B. W.; Darskus, R. *Anal. Chem.* **1997**, *69*, 601−606.
(23) Llompart, M. P.; Lorenzo, R. A.; Cela, R. *J. Chromatogr., A* **1996**, *723*, 123−134.
(24) Lancas, F. M.; Queiroz, M. E. C.; Silva, I. C. E. *Chromatographia* **1995**, *40*, 421−424.

S0003-2700(97)01185-2 CCC: $15.00 © 1998 American Chemical Society
Published on Web 04/18/1998

to the matrix−fluid interface and the process of analyte partitioning at the matrix−fluid interface. Optimization of extraction conditions can be determined through investigation of analyte−matrix interaction. Langenfeld et al.[26] successfully applied this model to interpret real-world sample extractions. Clifford et al.[27] proposed a model for a dynamic SFE process. In addition, several works[28−30] have involved directly correlating supercritical fluid chromatography (SFC) data with SFE. Although the SFE process has been considered much more complicated than the SFC process, they do share one common process: analytes are extracted or separated by partitioning, either between the matrixes and effluents or between stationary and mobile phases. One of the major differences is that analytes are scattered in the SFE extraction vessel, while a sample plug is injected into the top of the SFC column. Thus, parameters such as the capacity factor and peak broadening in chromatography should be related to extraction recovery in some way. McNally and Wheeler[28] predicted extraction efficiency using analyte capacity factors obtained from chromatograms. The SFC retention characteristics they found indeed reflected extraction recoveries to a certain extent. Lou et al.[30] examined the relationship between SFE and SFC using an extraction cell as the chromatographic column and derived a mathematical model based on convolution theory. They found that SFE elution profiles can be estimated from corresponding SFC peak shapes and capacity factors and successfully predicted extraction rates using chromatographic data for homogeneous samples, while providing helpful information about inhomogeneous samples.

In this study, we investigated the correlation between SFE and SFC in aqueous matrixes and aqueous stationary phases. Countercurrent chromatography (CCC) is appropriate for use with extraction and chromatography in liquid matrixes and stationary phases. CCC is a form of liquid chromatography. Since solid support for the stationary phase is not required, permanent adsorption of analytes does not occur. Separation is entirely attributable to partitioning of analytes between stationary and mobile phases. A fundamental study by Armstrong et al.[31] on separation efficiency over flow rate showed a convex curve, as compared with the regular concave van Deemter plot for packed-column chromatography. Large sample capacity makes CCC a good preparative technique. Applications include preparative separation of alkaloids,[32] purification of fish oil ethyl esters,[33] protein separation,[34] and chiral separation,[35] just to mention a few. Recently Weisz et al. introduced two novel techniques:[36,37] pH zone refining and pH zone focusing, which proved to be highly efficient for preparative separations. In addition to chromatography, the apparatus can be used as a very efficient extraction vessel.[38]

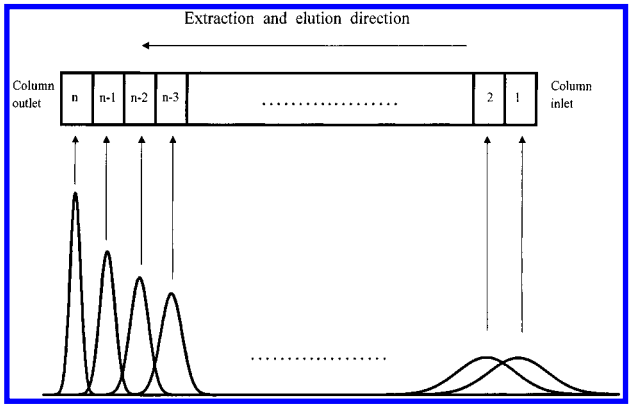

Figure 1. Theoretical model used in this study. The extraction cell was divided into limited layers, and the analyte was evenly distributed. During extraction, analytes in all layers were assumed to undergo chromatography. Accordingly, layers close to the column outlet gave relatively sharp peaks while those close to the column inlet gave relatively broad peaks, the broadest peak corresponding to the true chromatographic peaks that can be obtained by normal chromatographic process.

We recently[39,40] fabricated a CCC apparatus appropriate for using SF CO_2 as the mobile phase. This modified apparatus has the ability to perform both SFE and SFC with liquid matrixes and stationary phases in the same column and, thus, was appropriate for this study. A model was developed by dividing the extraction cell, i.e., the separation column, into finite layers. Each layer was considered as undergoing an independent chromatographic process. The recovery curves predicted using this model are compared with experimental data, and discrepancies observed between them are explained.

THEORY

The mechanism of supercritical fluid chromatography using liquid stationary phases involves completely pure partitioning of analytes in the mobile and stationary phases. Supercritical fluid extractions from liquid matrixes involve an identical situation in which enduring adsorption of analytes on matrixes simply does not occur. The liquid extraction vessel, i.e., the separation column, is evenly divided into *n* layers, as shown in Figure 1. During the extraction process, analytes in each layer are considered as undergoing independent chromatographic elution. Since the individual layers are located at different positions in the column, the resultant band broadenings vary with their corresponding retention times. In other words, analyte molecules in layers at the column inlet side should result in broader "peaks" than those at the column outlet side, due to longer retention times. Assuming Gaussian distribution of all peaks, the "imaginary" chromatographic peaks can all be derived from a single experimental chromatographic peak, as indicated below. A Gaussian distribu-

(25) Pawliszyn J. *J. Chromatogr. Sci.* **1993**, *31*, 31−37.
(26) Langenfeld J. J.; Hawthorne, S. B.; Miller, D. J.; Pawliszyn, J. *Anal. Chem.* **1995**, *67*, 1727−1736.
(27) Clifford, A. A.; Burford, M. D.; Hawthorne, S. B.; Langenfeld J. J.; Miller, D. J. *J. Chem. Soc.* **1995**, *91*, 1333−1338.
(28) McNally M. E. P.; Wheeler, J. R. *J. Chromatogr.* **1988**, *447*, 53−63.
(29) Furton K. G.; Lin, Q. *J. Chromatogr. Sci.* **1993**, *31*, 201−206.
(30) Lou, X.; Janssen, H.-G.; Cramers, C. A. *J. High Resolut. Chromatogr.* **1995**, *18*, 483−489.
(31) Armstrong, D. W.; Bertrand, G. L.; Berthod, A. *Anal. Chem.* **1988**, *60*, 2513−2519.
(32) Cooper, R. A.; Bowers, R. J.; Beckham, C. J.; Huxtable, R. J. *J. Chromatogr., A* **1996**, *732*, 43−50.
(33) Du, Q. Z.; Shu, A. M.; Ito, Y. J. *Liq. Chromatogr. Relat. Technol.* **1996**, *19*, 1451−1457.
(34) Shinomiya, K.; Muto, M.; Kabasawa, Y., Fales, H. M.; Ito, Y. *Liq. Chromatogr. Relat. Technol.* **1996**, *19*, 415−425.
(35) Ma, Y.; Ito, Y. *Anal. Chem.* **1995**, *67*, 3069−3074.
(36) Weisz, A.; Scher, A. L.; Shinomiya, K.; Fales, H. M.; Ito, Y. *J. Am. Chem. Soc.* **1994**, *116*, 704−708.
(37) Weisz, A.; Scher, A. L.; Ito, Y. *J. Chromatogr., A* **1996**, *732*, 283−290.
(38) Liu, Y.; Lopez-Avila, V.; Alcaraz, M. *Anal. Chem.* **1994**, *66*, 4483−4489.
(39) Yu, T.; Li, S.-E.; Chen, Y.-H.; Wang, H. P. *J Chromatogr.* **1996**, *724*, 91−96.
(40) Yu, T.; Chen, Y.-H. *J. Chromatogr., A* **1997**, *790*, 31−39.

tion of a chromatographic peak can generally be expressed as

$$y(t) = he^{-((t - t_R)^2/2\sigma^2)} \quad (1)$$

where y stands for the population (or the analyte mass) under the peak as a function of time t, h, the peak height, t_R, the peak retention time, and σ, the standard deviation. The Gaussian distributions for all the chromatographic elution of the "imaginary" layers can thus be expressed as

$$y_i(t) = h_i e^{-((t - t_{R_i})^2/2\sigma_i^2)} \qquad i = 1, ..., n \quad (2)$$

The plate height, H, of the column is defined as

$$H = \sigma^2/L \quad (3)$$

where σ is the standard deviation for the real chromatographic peak and L is the column length. Assuming the plate height, H, remains constant throughout the separation column if the SF CO_2 pressure drop is negligible, then the peak standard deviation for each layer can be determined by L_i, the distance from the column outlet to the head of layer i, as expressed in the following equation:

$$\frac{\sigma_1^2}{L_1} = \frac{\sigma_2^2}{L_2} = \frac{\sigma_3^2}{L_3} = \frac{\sigma_4^2}{L_4} = ... = \frac{\sigma_n^2}{L_n} \quad (4)$$

where σ_i is the standard deviation for each layer and L_i are given by

$$L_i = L\left(1 - \frac{i-1}{n}\right) \qquad i = 1, ..., n \quad (5)$$

Combining eqs 4 and 5 yields

$$\sigma_i^2 = \sigma_1^2\left(1 - \frac{i-1}{n}\right) \qquad i = 1, ..., n \quad (6)$$

Retention times for all the peaks can be derived as linear functions of the elution distances of the supercritical fluid:

$$t_{R_i} = t_{R_1}\left(1 - \frac{i-1}{n}\right) \qquad i = 1, ..., n \quad (7)$$

The standard deviations, σ's, of Gaussian chromatographic peaks for each layer can be expressed as

$$\sigma_i = A_i/h_i\sqrt{2\pi} \qquad i = 1, ..., n \quad (8)$$

where A_i stands for the integration of individual peak areas and h_i, the peak heights. Since analytes are distributed evenly in the column, the peak areas of all layers are therefore equal, and can be expressed as

$$A_1 = A_2 = ... = A_n = A/n \quad (9)$$

where A represents the total mass of the analyte in the sample. A_1, h_1, and t_1 can be obtained via actual chromatographic experiments. The standard deviation, σ_1, for the actual chromatographic peak can then be calculated using eq 8. Standard deviation, retention time, and peak height for each artificial layer can be computed from the actual chromatographic data using eqs 6−9. All these values are then plugged into eq 2 to calculate the individual population functions y_i for each divided layer. Figure 1 shows the Gaussian distributions of all layers. Layers at the column outlet exhibit sharp "peaks" while the first layer gives exactly the actual chromatographic peak (the broadest one in the series) obtained experimentally. Total analyte mass is equivalent to the summation of the areas under all the Gaussian peaks. Extraction recovery thus can be calculated by taking the quotient of the summation of y_i divided by the total area as a function of time, as in the following equation:

$$r(t) = \sum_i y_i(t)/A \quad (10)$$

Finally, the integration of on-line extraction signals as a function of time yielded the experimental recovery curve, which was then compared with the calculated data described above.

EXPERIMENTAL SECTION

Reagents and Sample Solutions. All extraction solutions were prepared in water obtained from a three-stage Milli-Q purification system. Acetophenone (+99%) and naphthalene (+99%) were purchased from Sigma (St. Louis, MO), benzaldehyde (+99%) was from Aldrich (Milwaukee, WI), and *m*-cresol (98%) and 2-naphthol (+99%) were from Riedel-de Haen (Seelze, Germany). HPLC-grade methanol was obtained from Mallinckrodt (Paris, KY). Extraction stock solutions (500 ppm) were prepared using water as the solvent and diluted to the desired sample concentrations thereafter. Nathphalene in methanol solution was spiked to the aqueous chromatographic samples. Since naphthalene is insoluble in water, it can be used as the SF CO_2 solvent front marker. SFC-grade CO_2 was purchased from Scott Specialty Products (Plumsteadville, PA).

Apparatus. A schematic diagram of the experimental setup is shown in Figure 2. The slowly rotating laboratory-made coil assembly housed in an oven was originally designed by Ito and Bhatnagar[41] and is described in detail elsewhere.[39,40] The separation column (i.e., the extraction vessel) was mounted solar-coaxially and wound from 4.40-m-long, 6.35-mm ($^1/_4$ in.)-o.d., 5.33-mm (0.210 in.)-i.d. nickel tubing on a 9-cm-radius column holder. Its total volume was about 95 mL. All connection tubes were PEEK tubing of 1.59 mm ($^1/_{16}$ in.) o.d. and 0.25 mm (0.01 in.) i.d., able to withstand pressures up to 34.5 MPa (5000 psi), and flexible enough to survive the stress created by the antitwisting mechanism of the rotation assembly. The small i.d. tubing also helped reduce the system's dead volume. Needle valves were used for V3, V4, and V6 in order to better control flow rates. Two six-port valves (Rheodyne model 7010) were used for flow-path switching and sample injection. All valves were connected using high-pressure fittings to ensure reliable operation. A 1-mL phase separator was installed before the detector to prevent the water droplets occasionally carried out by the SF CO_2 from getting into

(41) Ito, Y.; Bhatnagar, R. *J. Chromatogr.* **1981**, *207*, 171−180.

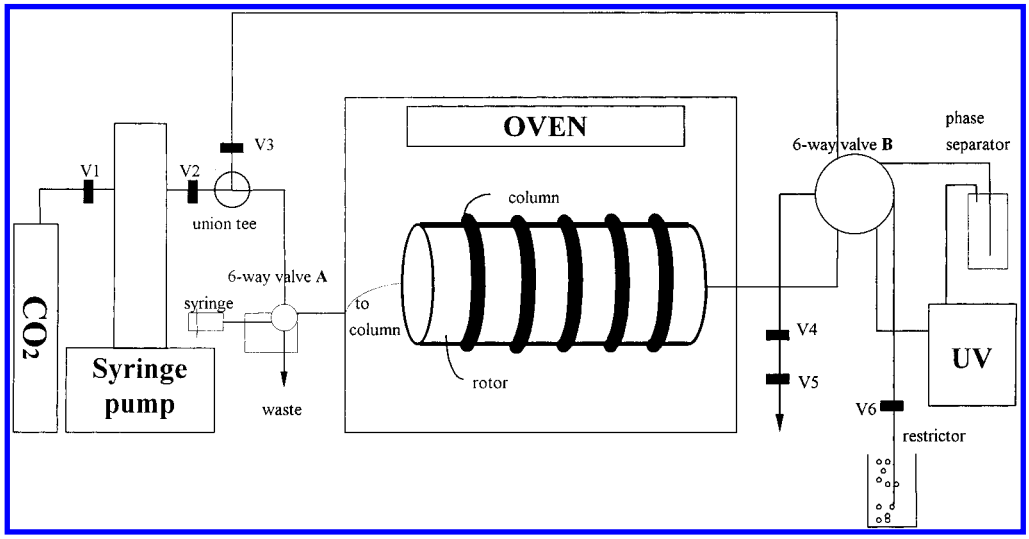

Figure 2. Schematic diagram of the experimental setup.

the monitor. A piece of 360-μm-o.d. and 50-μm-i.d. fused-silica tubing attached to the outlet of valve V6 served to provide back pressure. An Isco (Lincoln, NE) model 260D syringe pump was employed to deliver the SF CO_2 and a Perkin-Elmer (Norwalk, CT) photodiode array 235C detector was used to monitor the effluent.

Stationary-Phase Retention. Large stationary-phase capacity is one of the characteristics of CCC. Phase retention ratios in conventional CCC are subject to experimental conditions, such as the solvent system used, flow rate, and rotation speed. Temperature and pressure have been shown to be additional factors[39,40] when SF CO_2 is used as the mobile phase. Whenever CCC apparatus is employed in chromatographic applications, higher phase retentions are usually sought in order to obtain better peak resolutions. As for extraction, the phase retention upper limit apparently determines the maximum liquid sample volume allowed in the column; therefore, phase retention was also investigated in this study.

Valve V3 was always closed during the phase retention experiments. The oven was set to the desired temperature and the syringe pump filled with water. Water was then pumped to fill the column with valves V2, V4, and V5 open. The injected volume measured at the pump head was recorded as T just as water appeared at V5. Valves V2, V4, and V5 were then closed, and excess water in the pump was discarded. Liquid CO_2 was withdrawn from the cylinder to the pump and compressed to the desired pressure. The rotor motor was started and set to the experimental speed. Valves V2 and V4 were then opened and the flow rate was adjusted using the metering valve V5. Water was gradually displaced by SF CO_2 and collected in a graduated cylinder. Ten minutes after the SF CO_2 first appeared at the outlet, V4 was closed again. The volume of collected water was measured as T_1. Finally, residual water was removed with SF CO_2 while the column was stationary. The volume of removed water was measured, as T_2. The sum of T_1 and T_2 was compared with T to validate the total column volume and to eliminate volume measurement uncertainty. The quotient of T_2/T gave the phase retention ratio, S_F.

Extraction and Chromatography. The Swagelok union connecting the column and the outlet PEEK tubing was opened. An aqueous sample was injected at the column outlet using a 100-mL epidermal syringe not shown in the setup illustration. At the experimental temperature, SF CO_2 was delivered to the column when six-way valve B was set to break the connection between the column outlet and any openings. Several minutes later, after the entire system reached a stable pressure, the rotor was started at the desired speed, i.e., 80 rpm (see Results and Discussion). It took about 50 min for hydrodynamic equilibrium to occur. Ten minutes before continuous extraction began, i.e., about 40 min after the rotor was started, six-way valve A was closed to break the connection between the pump and the column and V3 was opened in order to let the SF CO_2 flow pass the UV monitor while keeping it under operational pressure. This avoided creating anomalous signals due to pressure surges when continuous extraction was begining. Ten minutes later, valve V3 was closed and six-way valve A was set to connect the pump and the column again. At this moment, continuous extraction was started by switching six-way valve B to allow flow past the phase separator, then the monitor, and finally to the outlet valve V6 attached as shown to a fused-silica restrictor that kept the flow rate at 0.7 mL/min. Aqueous sample (40 mL) at a concentration of 10 ppm were used in the experiments. Once extraction was completed, a 100-μL liquid sample was injected from valve A to start a chromatographic run. The sample concentrations of acetophenone, benzaldehyde, *m*-cresol, and 2-naphthol were 500, 400, 2000, and 500 ppm, respectively.

RESULTS AND DISCUSSION

Pressure drops were measured at the column head and tail under normal operating conditions. At 130 bar, no pressure difference was observed; at 100 bar, a difference of less than 1 bar was detected. At such small pressure drops, the plate height can be considered a constant, as assumed in the theoretical calculation, throughout the entire column.

Stationary-Phase Retention. Stationary-phase retention is considered one of the major parameters affecting CCC resolution and usually receives more research attention. However, only a nominal phase retention volume was required for our study, so comprehensive investigation was not conducted. Stationary-phase retention for various rotor speeds was examined at 130 bar and

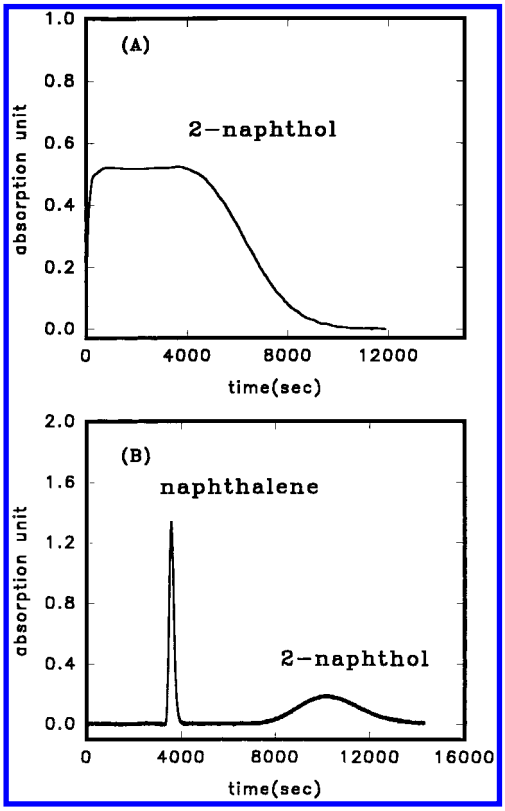

Figure 3. Extraction (A) and chromatographic (B) results for 2-naphthol. Experimental conditions: 100 bar, 40 °C.

50 °C, with an SF CO_2 flow rate of 0.7 mL/min. The maximum phase retention volume was reached at 80 rpm under the experimental conditions given above; therefore, extraction and chromatography experiments were all performed at this speed.

Preliminary Results. In this study, various experimental and extraction conditions were performed to investigate the performance of the proposed model over a broad range. The aqueous sample volume was kept constant during all measurements for case of comparison. Although the maximum stationary-phase volume can be as high as 55 mL at 130 bar and 50 °C, 40-mL samples were used under all experimental conditions. We were therefore able to avoid phase bleeding, which could occur when system pressures and temperatures were changed.

Typical extraction and chromatographic results, for example, for sample 2-naphthol, are shown in Figure 3. Note that the extraction was considered to start when hydrodynamic equilibrium was reached and the SF CO_2 flow was pumped continuously into the system. The calculated and the experimental recovery curves are shown in Figure 4. Acetophenone extraction and chromatography were also investigated, and the recovery curve is shown in Figure 5. Considerable deviations are evident in both sets of results: those for 2-naphthol with a large k' (1.847), and those for acetophenone with a small k' (0.097). Note that the experimental recovery slopes in both cases were steeper than calculated, and extraction was actually completed much earlier than predicted. This implies that analyte concentrations were higher at the column outlet than at the column inlet. In other words, analyte distributions were no longer uniform after the system reached hydrodynamic equilibrium. Accordingly, the model was modified in the following ways.

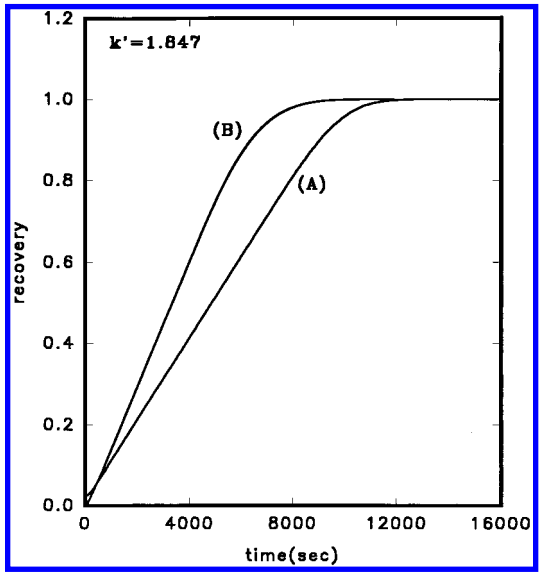

Figure 4. (A) Extraction recovery curve predicted from the chromatographic data. (B) Experimental extraction recovery curve for 2-naphthol. Experimental conditions: 100 bar, 40 °C; $K' = 1.847$.

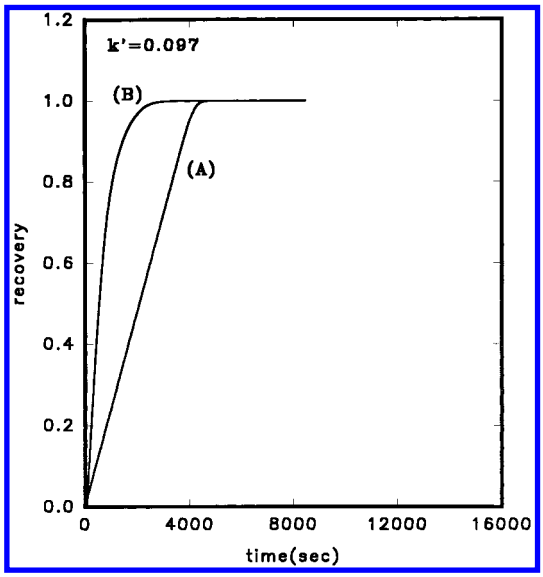

Figure 5. (A) Extraction recovery curve predicted from the chromatographic data. (B) Experimental extraction recovery curve for acetophenone. Experimental conditions: 130 bar, 50 °C; $K' = 0.097$.

Concentration Gradient. Note that the current model should take effect only when the pressure of SF CO_2 was same throughout the column according to our assumption, i.e., after the solvent system reached hydrodynamic equilibrium. When the SF CO_2 came into contact with the sample solutions, analyte concentrations were uniformly distributed. However, by the time the SF CO_2 reached the column outlet, the concentration distributions had changed. In fact, we did not realize this discrepancy in the first place until experimental data displayed it. Accordingly, concentration redistribution had to be resolved before the model could be considered complete.

In the extraction experiments, aqueous samples were injected into the column from the column outlet, while SF CO_2 was pumped into the column from the head. Therefore, sample solutions and SF CO_2 were separated. When rotation began, two fluids started flowing through each other as illustrated in Figure 6. At first, SF

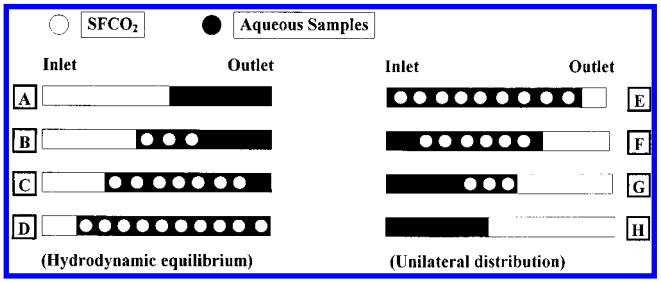

Figure 6. Schematic diagram of formation of hydrodynamic equilibrium and unilateral distribution due to flow-through of SF CO_2 and sample solution.

CO_2 occupied the inlet portion, while the sample solutions were located in the outlet—shown as stage A in Figure 6. One of the fluids (say, SF CO_2) formed droplets and moved toward the tail, displacing the other fluid. Finally, both fluids reached hydrodynamic equilibrium, indicated as stage D in Figure 6. From then on, sample solution was not removed from the column tail when both ends were open and SF CO_2 was being pumped in from the inlet end. However, if the flow-through continued with both ends closed, the two fluids would be separated completely into a so-called unilateral distribution,[42] indicated as stage H in Figure 6.

The concentration gradient thus formed can be estimated by an approach similar to countercurrent distribution (CCD) using k' values obtained from chromatograms. CCD was introduced by Craig et al.[43,44] in order to study an analogue of partition chromatography. In principle, it can be used to resolve solute concentration distributions for discrete stage extraction, such as occurs in a series of separation funnels. CCD assumes true analyte equilibrium distributions at each stage while prohibiting phase mixing in adjacent stages; i.e., longitudinal diffusion of analytes is prevented. The CCD formula was derived under conditions in which samples were introduced only into the top stage. But in our case, the sample solutions were spread evenly through all stages. Assume the total amount of analyte is Q. Since the column is divided into n layers, the quantity in each layer is simply Q/n. The capacity factor k' is defined as

$$k' = Q_s/Q_m \tag{11}$$

where Q_s is the quantity of analyte in the stationary phase and Q_m the quantity of analyte in the mobile phase. When the SF CO_2 and sample solutions started passing through each other, the analyte was distributed over the stationary and mobile phases. The total analyte quantity remaining in the stationary phase of the first layer after the mobile phase has passed the first layer can be expressed as

$$Q'_{s(1)} = \frac{Q}{n}\frac{Q_s}{Q_m + Q_s} = \frac{Q}{n}\frac{k'}{1 + k'} \tag{12}$$

The analyte quantity carried by the mobile phase to the second layer can be expressed as

$$Q'_{m(2)} = \frac{Q}{n}\frac{Q_m}{Q_m + Q_s} = \frac{Q}{n}\frac{1}{1 + k'} \tag{13}$$

These equations provide the basic calculations that enabled us to determine the analyte fractions as the fluids flowed through each other. As this process continued, the total analyte quantity could be calculated using the following formula:

$$Q'_{(i)} = Q_{(i)}\frac{k'}{1 + k'} + Q_{(i-1)}\frac{1}{1 + k'} \tag{14}$$

where $Q'_{(i)}$ is the total analyte quantity (including those in both mobile and stationary phases) remaining in the ith layer after the SF CO_2 has passed the ith layer, $Q_{(i)}$ is the total analyte quantity when the SF CO_2 arrived at the ith layer, and $Q_{(i-1)}$ is the total analyte quantity in the $(i - 1)$th layer. In other words, when the SF CO_2 had moved to the $(i + 1)$th layer, the total analyte quantity in the ith layer was equal to the amount left in the stationary phase (first term on the right-hand side of the equation) plus the amount carried over from the $(i - 1)$th by the mobile phase (second term on the right-hand side of the equation). Iterative calculations using eq 14 gave the analyte distribution when the flow-through was completed. A simple example is given in Table 1 to demonstrate how this repetitive process works.

Concentration redistributions of acetophenone and 2-naphthol were carried out, in which SF CO_2 passed through the sample solution and reached the column outlet, using the above approach. The results are illustrated in Figure 7. Analyte masses of both samples will accumulate in the outlet portion, but acetophenone with its smaller k' value accumulated more noticeably. Note that the extraction curve for 2-naphthol (see Figure 3A) forms a long plateau before falling; this matches the calculated concentration distribution, clearly demonstrating the necessity for modifying the original model. Once the analyte concentration distribution was corrected, a simple modification was made by multiplying the term $y_i(t)$ in eq 10 by the analyte mass fraction. The rest of the calculations was carried out the same way as before.

Recovery Curve Calculation Using Modified Model. The extraction column was divided into finite "imaginary" layers in our model. Analyte molecules in each layer were taken as a sample plug injected to the column and underwent chromatographic process. This best approximates the actual chromatographic process when the number of layers (n) approaches infinity. However, as n is increased, the computing time also increases very rapidly. Therefore, recovery curves as a function of layer number were examined. As n became greater and greater, the curve gradually converged to a limit. All computations were carried out using 900 layers after careful evaluation. Calculations involving the unmodified model yielded similar outcomes; therefore, these are not discussed in detail.

The 2-naphthol and acetophenone chromatograms were recalculated using the modified model. The results are shown in Figures 8 and 9, respectively. Significant improvements were achieved with 2-naphthol, although an apparent deviation between the experimental and predicted curves persisted for acetophenone, they matched notably better than before. Note that the 2-naphthol ($k' = 1.847$) sample yielded better outcomes than those of

(42) Ito, Y.; Bhatnagar, R. *J. Liq. Chromatogr.* **1984**, *7*, 257−273.
(43) Craig, L. C.; Post, O. *Anal. Chem.* **1949**, *21*, 500−504.
(44) Craig, L. C.; Hausman, W.; Ahrens, E. H., Jr; Harfenist, E. J. *Anal. Chem.* **1951**, *23*, 1236−1244.

Table 1. Example of Concentration Distribution Calculations during Flow-Through of SF CO_2 and Sample Solution[a]

layer no.	original fraction in each layer	the layer number SF CO_2 flow front reached				
		1	2	3	4	5
1	0.2	0.2	$0.2S = 0.16$	$0.16S = 0.128$	$0.128S = 0.1024$	$0.1024S = 0.08192$
2	0.2	0.2	$0.2 + 0.2M = 0.24$	$0.24S + 0.16M = 0.224$	$0.224S + 0.128M = 0.2048$	$0.2048S + 0.1024M = 0.18432$
3	0.2	0.2	0.2	$0.2 + 0.24M = 0.248$	$0.248S + 0.224M = 0.2432$	$0.2432S + 0.2048M = 0.23552$
4	0.2	0.2	0.2	0.2	$0.2 + 0.248M = 0.2496$	$0.2496S + 0.2432M = 0.24832$
5	0.2	0.2	0.2	0.2	0.2	$0.2 + 0.2496M = 0.24992$

[a] Assume the extraction column is divided into five layers and $k' = 4$, then $S = k'/(1 + k') = 0.8$ and $M = 1/(1 + k') = 0.2$. The table shows analyte fraction in each layer as the flow front moves toward the column outlet. The original fraction in each layer was 0.2. As SF CO_2 moved toward the column outlet, the fraction changed according to eq 14 (see text). Note that the calculated concentration profile is shown down the columns.

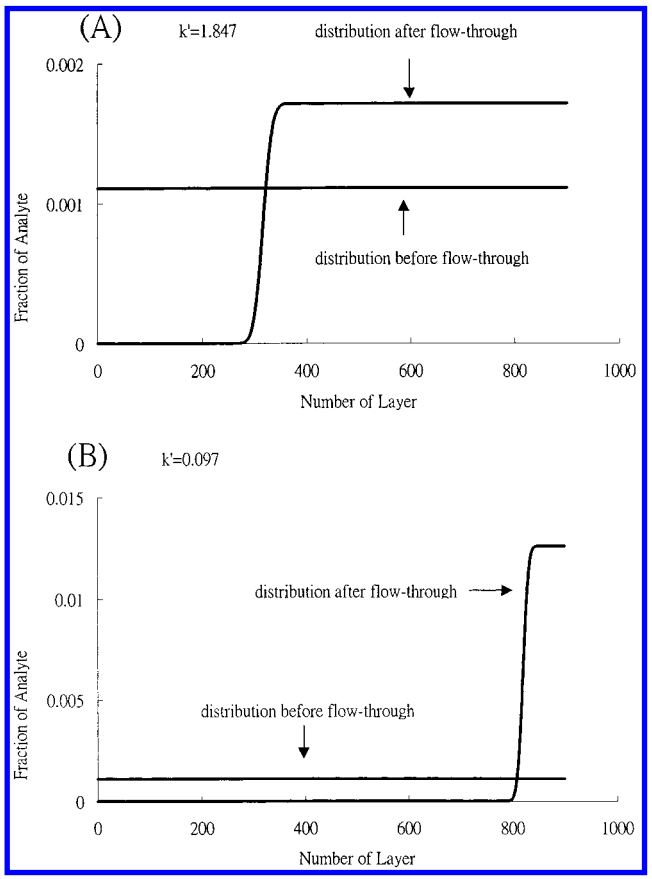

Figure 7. Concentration redistribution plots for (A) acetophenone and (B) 2-naphthol at the completion of flow-through of SF CO_2 and sample solution.

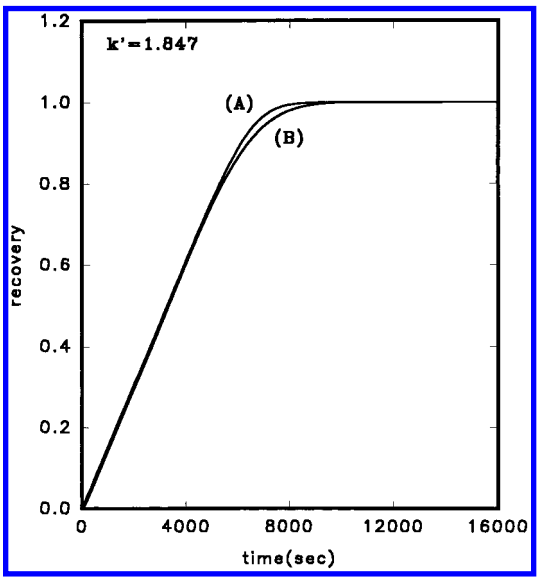

Figure 8. Extraction recovery curve for 2-naphthol using the modified model: (A) predicted curve; (B) experimental curve.

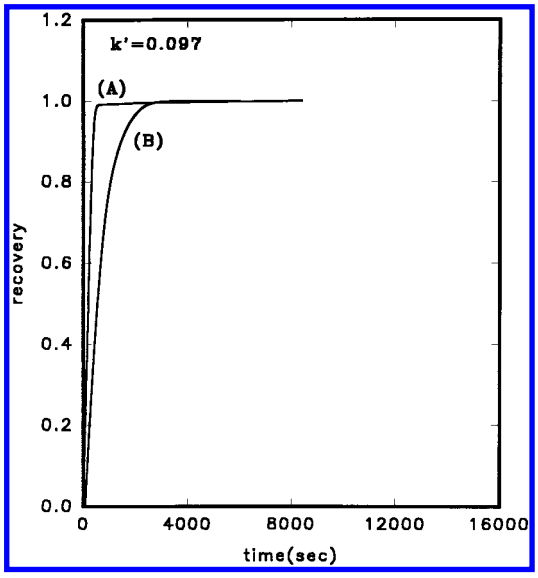

Figure 9. Extraction recovery curve for acetophenone using the modified model: (A) predicted curve; (B) experimental curve.

acetophenone ($k' = 0.097$) for both models. Thus, the effects of k' values on results warranted further investigation. Two more analytes, benzaldehyde and *m*-cresol, were added for this purpose. Experimental conditions were thus chosen in order to obtain chromatograms with different k' values. In fact, these data further confirmed the deviation trend; i.e., analytes with greater k' values have better predictive capacities. This deviation is more clearly demonstrated in Figure 10.

Chromatographic data from analytes with relatively large k' values yielded more satisfactory extraction recovery predictions. The final question remaining to be answered is why analytes with smaller k' values caused greater deviations. Recall the concentration redistribution computation during flow-through. The discrete layers of the extraction vessel were assumed to be completely separate and that true equilibrium between the fluids was reached in each stage. The actual situation apparently differed. In fact, true equilibrium could not occur during the process. The analyte mass dissolved and carried by the mobile phase must have been smaller than the calculated value. This is clearly demonstrated by Figures 8 and 9. Regardless of k' value, the simulated curves

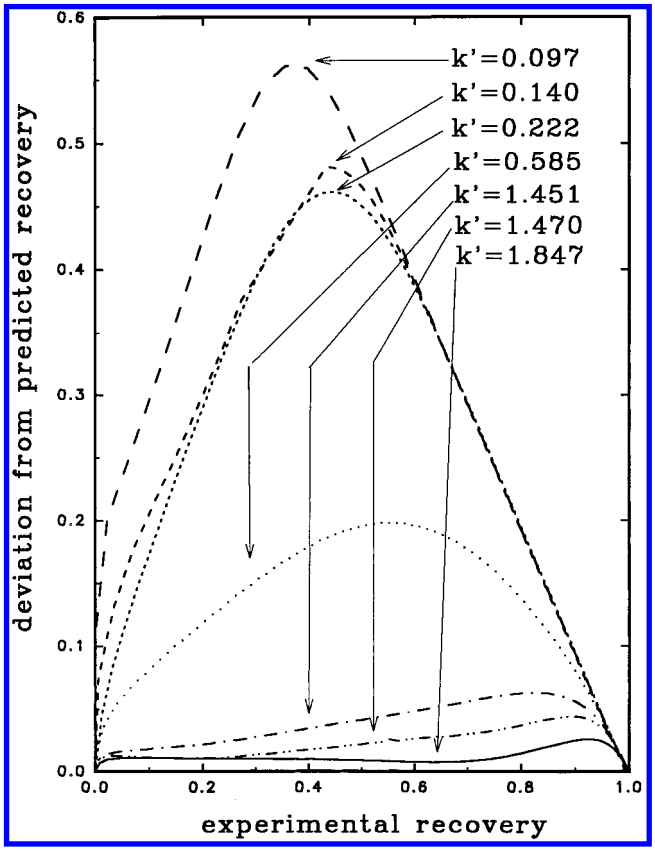

Figure 10. Deviation between the predicted and experimental recoveries as a function of the experimental recovery for seven trial runs at different k' values. Experimental conditions: for $k' = 0.097$, acetophenone, 130 bar, 50 °C; for $k' = 0.140$, benzaldehyde, 90 bar, 43 °C; for $k' = 0.222$, benzaldehyde, 100 bar, 50 °C; for $k' = 0.585$, benzaldehyde, 100 bar, 55 °C; for $k' = 1.451$, 2-naphthol, 130 bar, 50 °C; for $k' = 1.470$, *m*-cresol, 130 bar, 50 °C; for $k' = 1.847$, 2-naphthol, 100 bar, 40 °C.

always achieved complete extraction earlier than the experimental ones. In other words, positive deviations were always present (see Figure 10).

As noted above, the analyte masses accumulated rapidly near solvent fronts during the flow-through process. During the formation of concentration gradients, diffusion backward from the column outlet portion to the column inlet portion cannot to be ignored. However, longitudinal diffusion between layers was forbidden under our assumption. Accordingly, the concentration accumulation at the column outlet must have been further overestimated. This was especially pronounced for actophenone because of its relatively smaller capacity factor. According to Fick's law of diffusion, the particle flux in amount of molecules per unit area per unit time is

$$J = -D\,\mathrm{d}c/\mathrm{d}x \qquad (15)$$

where D is the diffusion coefficient and $\mathrm{d}c/\mathrm{d}x$ is the slope of the molar concentration. Apparently greater concentration differences caused by smaller capacity factors accounted for higher deviations by compounds with smaller k's. While further modification of the current model in support of this argument was not attempted, an experiment was designed to confirm this postulation. Extrac-

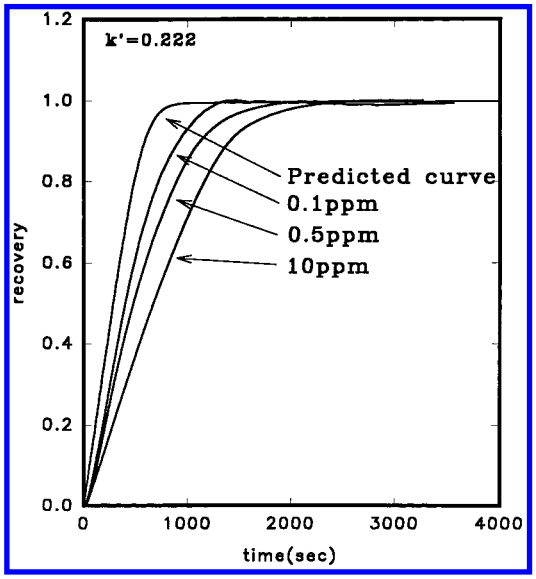

Figure 11. Predicted recovery curve compared with experimental results for different concentrations of benzaldehyde. Experimental conditions: 100 bar, 50 °C.

tions for three different concentrations (0.1, 0.5, and 10 ppm) of benzaldehyde samples were conducted under the same conditions, yielding a chromatographic capacity factor of 0.222. The results (see Figure 11) show that as the concentration decreased from 10 to 0.1 ppm the experimental results became closer and closer to the predicted curve. As pointed out above, benzaldehyde should accumulate quickly, as SF CO_2 moved toward the column outlet. Analyte diffusion back to the column inlet cannot be ignored in such cases. The experimental outcome for the higher concentration sample shifted further away from the predicted curve possibly due to the greater concentration difference created during the process.

CONCLUSIONS

Recovery curves for aqueous sample extractions using SF CO_2 were predicted using chromatographic data. The simulations were based on an artificial division of the extraction vessel into "imaginary" finite layers in which the chromatographies proceeded. The experimental data matched the predicted curves very well, for analytes with higher capacity factors. Deviations increased as capacity factors decreased. Although this deviation was not corrected by further modifying the theoretical model, the trend may be explained by excessively large longitudinal diffusions due to concentration gradients.

ACKNOWLEDGMENT

We thank A. C. Chang for his help with computer programming and K. P. Chang for manuscript preparation. Financial support (Grant NSC 86-2113-M-009-015) from the National Science Council of the Republic of China is also gratefully acknowledged.

Received for review October 24, 1997. Accepted March 4, 1998.

AC9711854